Letter

Broadband detection of 18 teeth in an 11-dB squeezing comb

Dennis Wilken,[1,2,*] Jonas Junker,[1,2,3] and Michèle Heurs[1]

[1] *Institute for Gravitational Physics, Leibniz University Hannover, D-30167 Hannover, Germany*
[2] *Max Planck Institute for Gravitational Physics (Albert Einstein Institute), D-30167 Hannover, Germany*
[3] *OzGrav, Centre for Gravitational Astrophysics, Research School of Physics & Research School of Astronomy and Astrophysics, Australian National University, Canberra, ACT, Australia*

(Received 14 July 2023; revised 31 January 2024; accepted 2 February 2024; published 4 March 2024)

Squeezed vacuum is a versatile resource of bipartite entanglement for quantum metrology and information. Optical parametric oscillators generate these states in a frequency comb structure. We show the simultaneous detection of 18 teeth with 11 dB of squeezing each. We built a 1.5-m-long optical resonator to increase the spectral teeth density and significantly increase the detection bandwidth by employing unbalanced homodyne detection instead of balanced. Our approach can be a crucial step in using the scaling potential of high-frequency squeezed states in quantum information.

DOI: 10.1103/PhysRevApplied.21.L031002

Squeezed states are continuous-variable (cv) quantum states featuring lower quantum uncertainty in one observable at the cost of higher uncertainty in the conjugate observable. Apart from applications in quantum metrology, such as the extension of detection range in gravitational wave detectors [1–3] or noise reduction in spectroscopy [4–6], squeezed states are used for applications in quantum information, including quantum random number generation [7], quantum key distribution (QKD) [8–10], entanglement swapping [11–13] and quantum teleportation [14–16]. A major limitation of squeezing is its vulnerability to optical loss which negatively impacts long-distance applications. In contrast to single-photon qubits, squeezed states can be generated and detected deterministically, which makes them highly attractive for cv quantum information processing [17].

Parametric down-conversion generates bipartite squeezed quantum states frequency-independently over multiple terahertz [18]. Squeezed light sources based on this process offer a unique scaling potential in the field of quantum information. Frequency multiplexing allows interaction with various entangled modes independently [19–23]. By introducing further temporal or spectral entanglement, these states can be extended to multidimensional cluster states which form a promising foundation for one-way quantum computing [24–28].

Single-pass squeezers without resonant enhancement of the squeezed field provide a continuous squeezing spectrum [29]. Still, the highest squeezing levels are obtained with optical resonators forming an optical parametric oscillator (OPO) [30–35]. These resonators exhibit longitudinal modes such that the squeezed output state has a frequency comb structure with a separation between the "teeth" corresponding to the resonator's free spectral range (FSR) [36].

Usually, balanced homodyne detectors are used to measure squeezed states under an arbitrary quadrature angle. However, high-quantum-efficiency (HQE) shot-noise-limited detectors are not fast enough to measure multiple FSRs over gigahertz frequencies. Three factors limit the bandwidth of balanced photodetectors: the photodiode's capacitance, the amplifier's bandwidth, and asymmetries between the photodiodes [37]. So far, the limited efficiency of broadband balanced detectors has prevented measuring more than 2 dB of squeezing at gigahertz frequencies [23,38,39]. Therefore, alternative methods such as bichromatic detection [33,40–42] or parametric amplification [18,43–45] are usually employed.

In this paper we use a different approach, demonstrating broadband homodyne detection of 18 teeth of a squeezing comb within a span of 3.6 GHz. We measured 11.1 dB of squeezing (up to 9.3 dB without dark noise subtraction) using a two-track approach. Firstly, we built an OPO with a roundtrip length of 1.5 m, corresponding to an FSR of only 200 MHz. Secondly, we implemented an unbalanced homodyne detection scheme drastically increasing the detector's bandwidth compared to our balanced design. Compared to previous reports on broadband homodyne detection [23,38,39,46], our results are a milestone achievement.

*dennis.wilken@aei.uni-hannover.de

Our squeezed light source offers a versatile resource for the field of quantum information. Implementing long squeezers allows the detection of more than 10 times the number of sideband modes compared to compact linear designs. This approach enables easy up-scaling for applications operating at small bandwidth or single frequency per resonance, such as multiplexed QKD [8,9,22] or one-way quantum computing [27,28].

Unbalanced detection [47] has been demonstrated previously for high-frequency measurements (3 dB squeezing and three teeth) but was described as a workaround solution as adequate balanced detectors were not available [46]. Still, designing a sufficiently balanced high-speed HQE detector remains a challenge; there is currently no technical or fundamental solution on the horizon. Therefore, focusing on unbalanced homodyne detection might be a key factor in exploiting the scaling potential of squeezed states, in particular when combined with long OPO resonators.

For balanced homodyne detection, the signal field $\hat{a}_\mathrm{s}$ is superimposed on a 50 : 50 beam splitter with a strong local oscillator $\hat{a}_\mathrm{lo}$ [48,49]. The two outputs are detected, and the photocurrents are subtracted. After decomposing the signal and local oscillator fields into constant terms $\bar{a}_\mathrm{s}$, $\bar{a}_\mathrm{lo}$ and time-varying terms $\delta\hat{a}_\mathrm{s}$, $\delta\hat{a}_\mathrm{lo}$, the fluctuating photocurrent of a balanced setup reads

$$\delta\hat{I}_\mathrm{bal} \propto \frac{1}{2}\left(\bar{a}_\mathrm{lo}\delta\hat{X}_{\theta,\mathrm{s}} + \bar{a}_\mathrm{s}\delta\hat{X}_{-\theta,\mathrm{lo}}\right). \tag{1}$$

Here, the small $\delta\hat{a}^2$ terms are neglected and $\delta\hat{X}_\theta = \frac{1}{2}\left(\delta\hat{a}^\dagger e^{i\theta} + \delta\hat{a}e^{-i\theta}\right)$ describes the quadrature operator for the fluctuating field $\delta\hat{a}$ under an arbitrary readout angle θ. To fulfill the homodyne approximation, the local oscillator (LO) power needs to be much stronger than the signal ($\bar{a}_\mathrm{lo} \gg \bar{a}_\mathrm{s}$) such that $\bar{a}_\mathrm{s}\delta\hat{X}_{-\theta,\mathrm{lo}}$ can be neglected.

Work on high-speed, shot-noise-limited balanced detectors to measure squeezing at radio frequencies is the topic of ongoing research in the field. Sensors based on packaged components on printed circuit boards usually achieve bandwidths significantly below 1 GHz [50–53]. Higher bandwidth can be achieved using a higher level of integration employing photonic integrated circuits or custom amplifiers [38,54–57].

However, none of these detectors provides enough bandwidth and close to unity quantum efficiency to detect high levels of squeezing over many FSRs yet. The main bandwidth limitation of these balanced detectors arises from frequency-dependent electrical asymmetries or optical path length differences between the two ports of the detector. In this case, the photocurrents of the two photodiodes are not equally subtracted, causing a distorted quadrature measurement. These imperfections lead to a reduction in common-mode rejection ratio.

Balancing is a technical challenge that gets increasingly difficult with bandwidth. We circumvented the bandwidth limitation of balanced detection using a single-photodiode detector. For a homodyne measurement on a beam splitter with amplitude reflectivity r and transmissivity t, the fluctuating current of a single photodiode reads

$$\delta\hat{I}_\mathrm{sing} \propto t\bar{a}_\mathrm{lo}r\delta\hat{X}_{\theta,\mathrm{s}} + t^2\bar{a}_\mathrm{lo}\delta\hat{X}_{1,\mathrm{lo}} + r\bar{a}_\mathrm{s}t\delta\hat{X}_{-\theta,\mathrm{lo}} + r^2\bar{a}_\mathrm{s}\delta\hat{X}_{1,\mathrm{s}}, \tag{2}$$

with amplitude quadrature $\delta\hat{X}_{\theta=0} = \delta\hat{X}_1$. Compared to the balanced case, there is no noise suppression eliminating $\delta\hat{X}_1$ terms. Even without classical noise, these terms carry vacuum fluctuations and act as a loss channel for the squeezing with losses equal to t^2. Therefore, we have chosen a power transmission of only 1% to avoid strong degradation of the squeezed state at the cost of increasing the demand for LO power.

In our experiment, amplitude quadrature noise suppression is not required. We utilize an optically pumped solid-state laser that is shot noise limited a few megahertz above its relaxation oscillation at about 1 MHz [58]. However, it is crucial to select carefully and, if necessary, stabilize the laser source when applying our approach in a different setup.

To acquire a signal for phase control, we displace our signal with a bright but weak seed field. Opposed to the balanced case, the interference between this seed field and the LO changes the shot noise level. This can be avoided by maintaining a constant photocurrent through adjustments to $\bar{a}_\mathrm{lo}$ (applied here) or $\bar{a}_\mathrm{s}$ or by alternatively using a frequency-shifted control field [59].

Our squeezing comb is generated using a subthreshold OPO with an optical roundtrip length of 1.5 m, arranged in a folded bow-tie layout corresponding to an FSR of 200 MHz as illustrated in Fig. 1. The resonator consists of a closed aluminum spacer with a partially reflective coupler with an 81.7% reflectivity, along with five high-reflective (HR) mirrors and a type-0 periodically-poled potassium titanyl phosphate (PPKTP) crystal. The pump light is produced by a similar four-mirror second harmonic generation (SHG) resonator with a coupler reflectivity of 90%. For the measurement presented, a pump power of 846 mW at 532 nm was utilized. A stable nonplanar ring oscillator Nd:YAG laser by Coherent operating at the fundamental wavelength of 1064 nm serves as the laser source, which is amplified to 4 W using a neoVAN-2s amplifier by neoLASE.

The squeezing comb is measured by superimposing it with a LO on a 99 : 1 beam splitter and detecting the combined beams on an rf photodetector ($\mathrm{PD_{det}}$) developed in-house. It is based on a HQE photodiode with 80-μm active diameter (manufactured by Laser Components), which detects an optical power of 8.7 mW. Using a bias tee, the detector splits the signal into a low-frequency dc stage

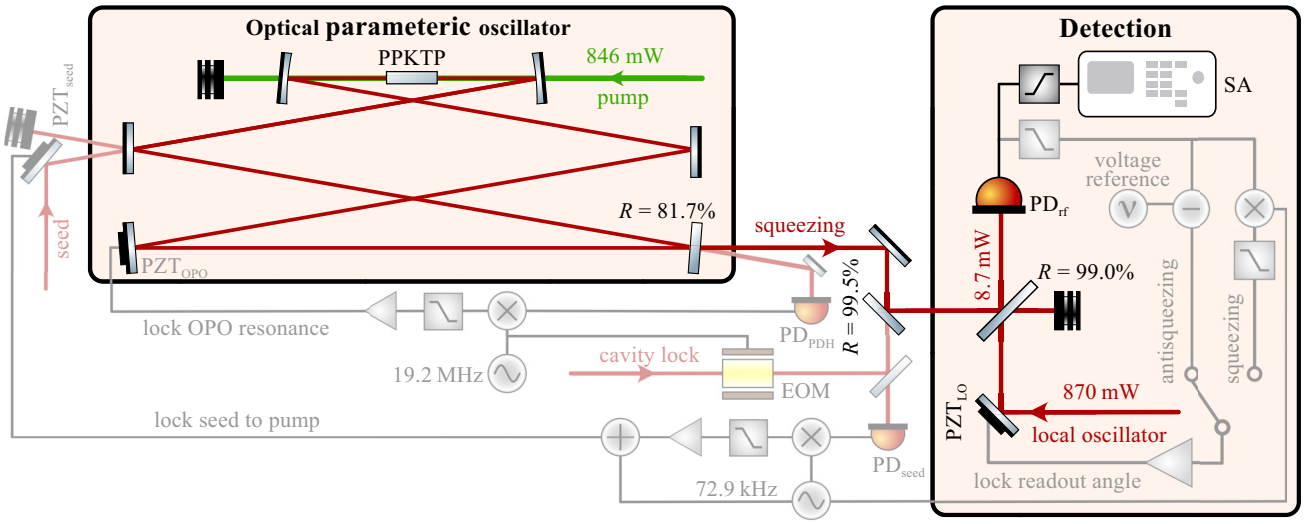

FIG. 1. Schematic of the generation and detection of the squeezing comb. Grayed-out components show the fields and control loops for resonator length and phase control. The OPO has a roundtrip length of 1.5 m, corresponding to an FSR of approximately 200 MHz. The readout quadrature phase θ is adjusted by PZT_{lo}. SA, spectrum analyzer; EOM, electro-optical modulator; PD, photodetector; PZT, piezoelectric phase shifter.

and a high-frequency ac stage employing commercial transimpedance and rf amplifiers. A detailed publication on the detector is currently under preparation.

Several control loops are implemented to stabilize the roundtrip length of the resonators and the phase relations of the fields. The SHG and OPO are locked using the Pound-Drever-Hall (PDH) technique [60]. The PDH control field for the OPO is injected in the opposite direction to the squeezing via a pickoff mirror with $R = 99.5\%$. To control the phase of the squeezing, a phase-modulated seed field (a_s) with a frequency of 72.9 kHz is injected through an HR mirror. The deamplification of the seed field in the crystal is monitored by PD_{seed} and the phase is controlled using a lock-in scheme accordingly. The seed field interferes with the LO on the homodyne detector. After demodulation, this allows locking to the amplitude quadrature (destructive interference), or the phase quadrature (mid-fringe) after subtracting a reference voltage (see Fig. 1). The rf output is measured with a Keysight N9020a spectrum analyzer. The shot noise reference is recorded with the squeezing path blocked.

The measured squeezing comb is depicted in Fig. 2. It consists of individual data sets for the single teeth separated by the FSR of 199.47 MHz merged into a full-band measurement. The raw data are presented in (a). After subtracting the electronic dark noise and normalizing the data to shot noise, the comb exhibits periodic behavior with constant squeezing and antisqueezing values (b). Three exemplary teeth are presented in (c). An animation of all teeth is shown in Video 1.

To see the full potential of our squeezing source, we subtract the dark noise contribution from our squeezing measurement. The squeezing levels (red trace) are often below the dark noise. Accordingly, subtracting dark noise makes the squeezing traces noisier (compare to the light red trace). Therefore, we conducted additional 2-second zero-span measurements to determine the squeezing levels more precisely. We measured an average squeezing of 11.1 ± 0.2 dB squeezing and an average anti-squeezing of 19.2 ± 0.1 dB across all teeth. The error margin corresponds to the standard deviation of these values. The higher fluctuation of the squeezing values is most likely explained by the influence of the dark noise but could also indicate frequency-dependent excess loss ($\leq 0.7\%$) [61]. Without dark noise subtraction, 9.3 dB of squeezing was measured at the first FSR.

The performance of the setup can be characterized by the total efficiency and the phase noise. These values are acquired by fitting the spectra of the first FSR for different pump powers [62,63]. The total efficiency was determined to be 93.3%. The escape efficiency of the OPO is 98.7%, corresponding to a roundtrip loss of 0.23%. The propagation efficiency of the beam splitters and lenses was measured to be 98.5%, while the visibility's efficiency is 98.0%. Similar to [30], we determine the quantum efficiency (QE) of the detector to be at least 97.9%. These contributions are the basis for further improvements. From the same fit, we estimate the phase noise below 5 mrad. The contribution of the OPO's HR mirrors to the overall loss is negligible, suggesting the feasibility of constructing longer OPO cavities with additional mirrors and higher teeth density.

Some effects currently limit the detection, which can be overcome in the future. The measurement span is limited by the bandwidth of the spectrum analyzer. Recent

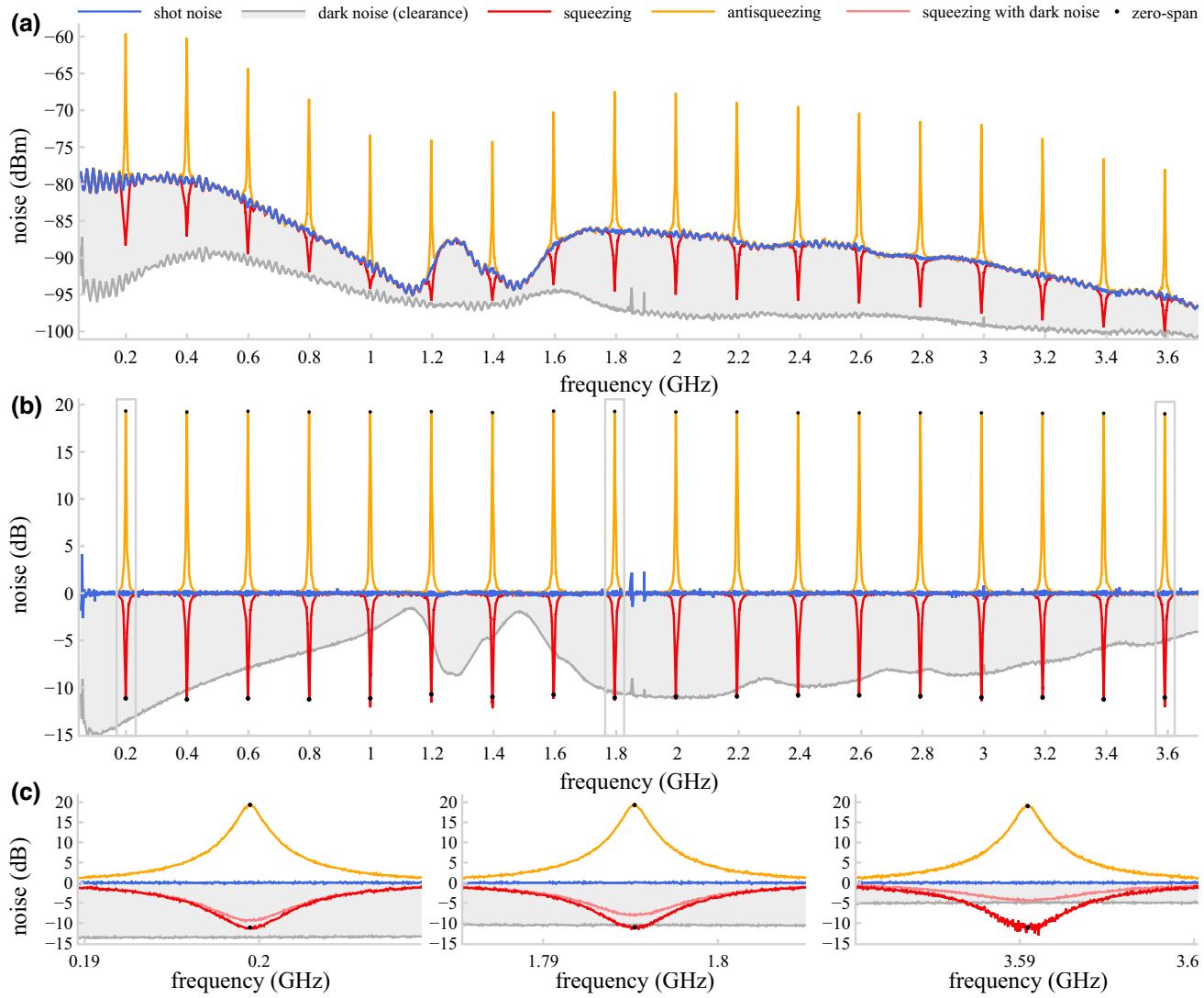

FIG. 2. Measurement of the squeezing comb. The raw data is presented in (a). The data is a combination of a full span measurement (span 3.65 GHz, resolution bandwidth (RBW) 1 MHz, video bandwidth (VBW) 200 Hz, sweep time 60 s) and individual measurements at each tooth (span 20 MHz, RBW 100 kHz, VBW 20 Hz, sweep time 30 s). (b) shows the measurement after normalization to shot noise and subtraction of the dark noise. Here, the gray line indicates the difference between shot noise and dark noise. Whenever the dark noise clearance is small, the squeezing trace broadens. In the full span picture, this is shown as varying squeezing levels. To reduce this effect, a rolling average over five points was applied. Furthermore, additional zero-span measurements (black dots) were performed to narrow down the measurement uncertainty. Three exemplary teeth measurements are displayed in (c), showing an additional squeezing trace without dark noise subtraction (light red). An animation of all individual teeth measurements is shown in Video 1.

measurements in our lab indicate shot-noise limitation up to 6.5 GHz. Furthermore, the necessity to subtract dark noise is a limiting factor and is often not possible in actual applications. The detector utilizes commercially available packaged components; a future iteration with a higher level of integration and customization could improve the dark noise clearance and increase the bandwidth, providing access to additional sidebands with a better signal-to-noise ratio.

In previous stages of this experiment, we used balanced homodyne detection and observed degradation of squeezing levels above 500 MHz. Early iterations of our balanced detector design were used for publications such as [23,39] observing reduced squeezing values at gigahertz frequency. Accordingly, we infer that these detectors were also limited by insufficient balancing. The same behavior was observed by [64].

Bichromatic homodyne detection with two LO frequencies at ± the measurement frequency is a common approach to measure squeezing over multiple gigahertz [33,40–42]. This optical demodulation enables measurements at gigahertz frequencies on a low-bandwidth

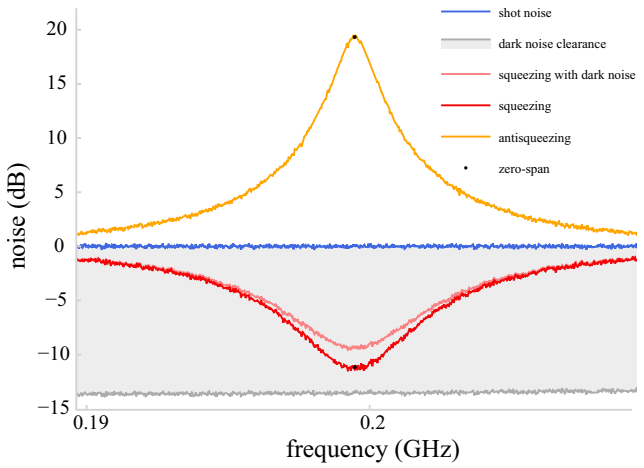

VIDEO 1. Animation of all 18 teeth of the squeezing comb after normalization to shot noise. Three teeth are shown in Fig. 2(c).

detector. While this approach reliably provides access to high frequencies, there are two drawbacks. First, measuring different frequency modes requires an adaptation of the LO's frequency. Second, the measurement cannot distinguish between a resonance's upper and lower side. An unbalanced bichromatic detection could measure a high number of modes simultaneously with the option of shifting the center frequency to higher modes. Still, the scheme could not differentiate between an upper or lower FSR.

A third option for measuring a squeezing comb is to amplify it phase-sensitively to a state well above the quantum regime using an optical parametric amplifier [18,43,44]. This allows for detection with lower-efficiency detectors without degradation of the squeezing level. Recently, a squeezing measurement combining parametric amplification and a commercial broadband balanced photodetector has been demonstrated, reaching 43 GHz bandwidth [45]. A similar measurement would be possible with an unbalanced commercial detector where a bandwidth surpassing 100 GHz seams in reach.

These two alternative methods enabled the detection of moderate levels of squeezing over high bandwidth and a large number of teeth [44,65]. Bichromatic detection allowed the detection of three sidebands of a 10-dB squeezing comb [33]. Our approach of combining unbalanced detection with long OPO enables us to measure both strong squeezing levels and many modes.

We demonstrated a long and efficient OPO resonator generating a squeezing comb with tooth separation of only 200 MHz and the broadband detection of 18 sideband pairs squeezed by 11.1 dB achieving a bandwidth of 3.6 GHz. Previously, broadband homodyne detection [23,38,39,46] was either limited by the balancing bandwidth or the efficiency to either low frequency or low squeezing values not exceeding 2 dB. Our solution circumvents the balancing problem while allowing the implementation of off-the-shelf HQE photodiodes.

High-speed and broadband detection will be a crucial factor in harnessing the scaling potentials of squeezing combs and spectral or temporal cluster states. While current research focuses on balanced schemes and is limited by either bandwidth or efficiency, we question this paradigm and encourage the investigation of unbalanced designs as a viable alternative. The balancing and efficiency issue will be challenging for years, and even with improvements achieved, unbalanced designs will remain faster than their balanced counterparts. Our scheme increases the number of accessible modes and potentially reduces the number of required detectors and demand for lossy demultiplexers in the field of quantum information. We have shown that long OPOs with low FSR are feasible, extendable, and an easy solution to increasing the number of accessible sideband modes.

Acknowledgments. This work was funded by the Deutsche Forschungsgemeinschaft (Excellence PhoenixD (EXC 2122, Project ID 390833453), Excellence QuantumFrontiers (EXC 2123, Project ID 390837967)).

[1] J. Lough *et al.*, First demonstration of 6 dB quantum noise reduction in a kilometer scale gravitational wave observatory, Phys. Rev. Lett. **126**, 041102 (2021).
[2] F. Acernese *et al.*, Increasing the astrophysical reach of the advanced Virgo detector via the application of squeezed vacuum states of light, Phys. Rev. Lett. **123**, 231108 (2019).
[3] A. Buikema *et al.*, Sensitivity and performance of the advanced LIGO detectors in the third observing run, Phys. Rev. D **102**, 062003 (2020).
[4] Y. Michael *et al.*, Squeezing-enhanced Raman spectroscopy, npj Quantum Inf. **5**, 1 (2019).
[5] M. Lassen *et al.*, Quantum-enhanced continuous-wave stimulated Raman scattering spectroscopy, Optica **7**, 470 (2020).
[6] E. Huntington *et al.*, High-precision cavity spectroscopy using high-frequency squeezed light, Opt. Express **29**, 6053 (2021).
[7] T. Michel *et al.*, Real-time source-independent quantum random-number generator with squeezed states, Phys. Rev. Appl. **12**, 034017 (2019).
[8] T. Gehring *et al.*, Implementation of continuous-variable quantum key distribution with composable and one-sided-device-independent security against coherent attacks, Nat. Commun. **6**, 1 (2015).
[9] L. S. Madsen *et al.*, Continuous variable quantum key distribution with modulated entangled states, Nat. Commun. **3**, 1 (2012).
[10] S. Pirandola *et al.*, Advances in quantum cryptography, Adv. Opt. Photonics **12**, 1012 (2020).
[11] R. E. Polkinghorne and T. C. Ralph, Continuous variable entanglement swapping, Phys. Rev. Lett. **83**, 2095 (1999).
[12] S. Takeda *et al.*, Entanglement swapping between discrete and continuous variables, Phys. Rev. Lett. **114**, 100501 (2015).
[13] X. Su *et al.*, Quantum entanglement swapping between two multipartite entangled states, Phys. Rev. Lett. **117**, 240503 (2016).
[14] A. Furusawa *et al.*, Unconditional quantum teleportation, Science **282**, 706 (1998).

[15] H. Yonezawa, T. Aoki, and A. Furusawa, Demonstration of a quantum teleportation network for continuous variables, Nature **431**, 430 (2004).

[16] M. Huo *et al.*, Deterministic quantum teleportation through fiber channels, Sci. Adv. **4**, eaas9401 (2018).

[17] S. Takeda and A. Furusawa, Optical hybrid quantum information processing, Lect. Notes Phys. **911**, 439 (2016).

[18] N. Takanashi *et al.*, All-optical phase-sensitive detection for ultrafast quantum computation, Opt. Express **28**, 34916 (2020).

[19] F. Li *et al.* Demonstration of fully-connected quantum communication network exploiting entangled sideband modes, Front. Phys. **18**, 1 (2023).

[20] Y. Wu *et al.*, Multi-channel multiplexing quantum teleportation based on the entangled sideband modes, Photonics Res. **10**, 1909 (2022).

[21] S. Shi *et al.*, Demonstration of channel multiplexing quantum communication exploiting entangled sideband modes, Phys. Rev. Lett. **125**, 070502 (2020).

[22] B. Hage, A. Samblowski, and R. Schnabel, Towards Einstein-Podolsky-Rosen quantum channel multiplexing, Phys. Rev. A **81**, 6230167 (2010).

[23] M. Heurs *et al.*, Multiplexed communication over a high-speed quantum channel, Phys. Rev. A. **81**, 032325 (2010).

[24] R. Raussendorf and H. J. Briegel, A one-way quantum computer, Phys. Rev. Lett. **86**, 5188 (2001).

[25] N. C. Menicucci *et al.*, Universal quantum computation with continuous-variable cluster states, Phys. Rev. Lett. **97**, 110501 (2006).

[26] N. C. Menicucci, S. T. Flammia, and O. Pfister, One-way quantum computing in the optical frequency comb, Phys. Rev. Lett. **101**, 130501 (2008).

[27] R. N. Alexander *et al.*, One-way quantum computing with arbitrarily large time-frequency continuous-variable cluster states from a single optical parametric oscillator, Phys. Rev. A **94**, 032327 (2016).

[28] B. H. Wu *et al.*, Quantum computing with multidimensional continuous-variable cluster states in a scalable photonic platform, Phys. Rev. Res. **2**, 023138 (2020).

[29] T. Kashiwazaki *et al.*, Fabrication of low-loss quasi-single-mode PPLN waveguide and its application to a modularized broadband high-level squeezer, Appl. Phys. Lett. **119**, 251104 (2021).

[30] H. Vahlbruch *et al.*, Detection of 15 dB squeezed states of light and their application for the absolute calibration of photoelectric quantum efficiency, Phys. Rev. Lett. **117**, 110801 (2016).

[31] F. Meylahn *et al.*, Squeezed states of light for future gravitational wave detectors at a wavelength of 1550 nm, Phys. Rev. Lett. **129**, 121103 (2022).

[32] J. Heinze *et al.*, Observation of squeezed states of light in higher-order Hermite-Gaussian modes with a quantum noise reduction of up to 10 dB, Phys. Rev. Lett. **128**, 083606 (2022).

[33] J. Wang *et al.*, Observation of a comb of squeezed states with a strong squeezing factor by a bichromatic local oscillator, Opt. Lett. **45**, 2419 (2020).

[34] K. Peng *et al.*, Detection and perfect fitting of 13.2 dB squeezed vacuum states by considering green-light-induced infrared absorption, Opt. Lett. **43**, 5411 (2018).

[35] M. S. Stefszky *et al.*, Balanced homodyne detection of optical quantum states at audio-band frequencies and below, Class. Quantum Grav. **29**, 145015 (2012).

[36] A. E. Dunlop *et al.*, Generation of a frequency comb of squeezing in an optical parametric oscillator, Phys. Rev. A - At., Mol., Opt. Phys. **73**, 013817 (2006).

[37] A. V. Masalov *et al.*, Noise spectra in balanced optical detectors based on transimpedance amplifiers, Rev. Sci. Instrum. **88**, 113109 (2017).

[38] J. F. Tasker *et al.*, Silicon photonics interfaced with integrated electronics for 9 GHz measurement of squeezed light, Nat. Photonics **15**, 11 (2020).

[39] T. Eberle *et al.*, Continuous-wave nonclassical light with gigahertz squeezing bandwidth, Opt. Lett. **37**, 2367 (2012).

[40] A. M. Marino *et al.*, Bichromatic local oscillator for detection of two-mode squeezed states of light, J. Opt. Soc. Amer. B **24**, 335 (2007).

[41] C. S. Embrey *et al.*, Bichromatic homodyne detection of broadband quadrature squeezing, Opt. Express **24**, 27298 (2016).

[42] B. Xie *et al.*, Quantum theory of phase-sensitive heterodyne detection, JOSA B **33**, 1365 (2016).

[43] Y. Shaked *et al.*, Lifting the bandwidth limit of optical homodyne measurement with broadband parametric amplification, Nat. Commun. **9**, 1 (2018).

[44] Y. Tian *et al.*, Cavity enhanced parametric homodyne detection of a squeezed quantum comb, Opt. Lett. **47**, 533 (2022).

[45] A. Inoue *et al.*, Toward a multi-core ultra-fast optical quantum processor: 43-GHz bandwidth real-time amplitude measurement of 5-dB squeezed light using modularized optical parametric amplifier with 5G technology, Appl. Phys. Lett. **122**, 104001 (2023).

[46] R. J. Senior *et al.*, Observation of a comb of optical squeezing over many gigahertz of bandwidth, Opt. Express **15**, 5310 (2007).

[47] S. Wallentowitz and W. Vogel, Unbalanced homodyning for quantum state measurements, Phys. Rev. A **53**, 4528 (1996).

[48] H. P. Yuen and V. W. Chan, Noise in homodyne and heterodyne detection, Opt. Lett. **8**, 177 (1983).

[49] J. H. Shapiro, Quantum noise and excess noise in optical homodyne and heterodyne receivers, IEEE J. Quantum Electron **QE-21**, 237 (1985).

[50] Q. Lu *et al.*, Ultra-low-noise balanced detectors for optical time-domain measurements, IEEE Trans. Nucl. Sci. **66**, 1048 (2019).

[51] T. Serikawa and A. Furusawa, 500 MHz resonant photodetector for high-quantum-efficiency, low-noise homodyne measurement, Rev. Sci. Instrum. **89**, 063120 (2018).

[52] D. Huang *et al.*, A 300-MHz bandwidth balanced homodyne detector for continuous variable quantum key distribution, Chin. Phys. Lett. **30**, 114209 (2013).

[53] R. Kumar *et al.*, Versatile wideband balanced detector for quantum optical homodyne tomography, Opt. Commun. **285**, 5259 (2012).

[54] X. Zhang *et al.*, 1.2-GHz balanced homodyne detector for continuous-variable quantum information technology, IEEE Photonics J. **10**, 1 (2018).

[55] D. Milovancev *et al.*, Chip-level GHz capable balanced quantum homodyne receivers, J. Lightwave Technol. **40**, 7518 (2022).

[56] B. Bai *et al.*, 18.8 Gbps real-time quantum random number generator with a photonic integrated chip, Appl. Phys. Lett. **118**, 264001 (2021).

[57] C. Bruynsteen *et al.*, Integrated balanced homodyne photonic–electronic detector for beyond 20 GHz shot-noise-limited measurements, Optica **8**, 1146 (2021).

[58] D. Ottaway *et al.*, Frequency and intensity noise of an injection-locked Nd:YAG ring laser, Appl. Phys. B **71**, 163 (2000).

[59] H. Vahlbruch *et al.*, Coherent control of vacuum squeezing in the gravitational-wave detection band, Phys. Rev. Lett. **97**, 11101 (2006).

[60] R. W. P. Drever *et al.*, Laser phase and frequency stabilization using an optical resonator, Appl. Phys. B Photophys. Laser Chem. **31**, 97 (1983).

[61] T. Serikawa and A. Furusawa, Excess loss in homodyne detection originating from distributed photocarrier generation in photodiodes, Phys. Rev. Appl. **10**, 064016 (2018).

[62] E. S. Polzik *et al.*, Atomic spectroscopy with squeezed light for sensitivity beyond the vacuum-state limit, Appl. Phys. B Photophys. Laser Chem. **55**, 279 (1992).

[63] T. Aoki *et al.*, Squeezing at 946 nm with periodically poled KTiOPO 4, Opt. Express **14**, 6930 (2006).

[64] T. Kashiwazaki *et al.*, Continuous-wave 6-dB-squeezed light with 2.5-THz-bandwidth from single-mode PPLN waveguide, APL Photonics **5**, 036104 (2020).

[65] M. Chen *et al.*, Experimental realization of multipartite entanglement of 60 modes of a quantum optical frequency comb, Phys. Rev. Lett. **112**, 120505 (2014).